

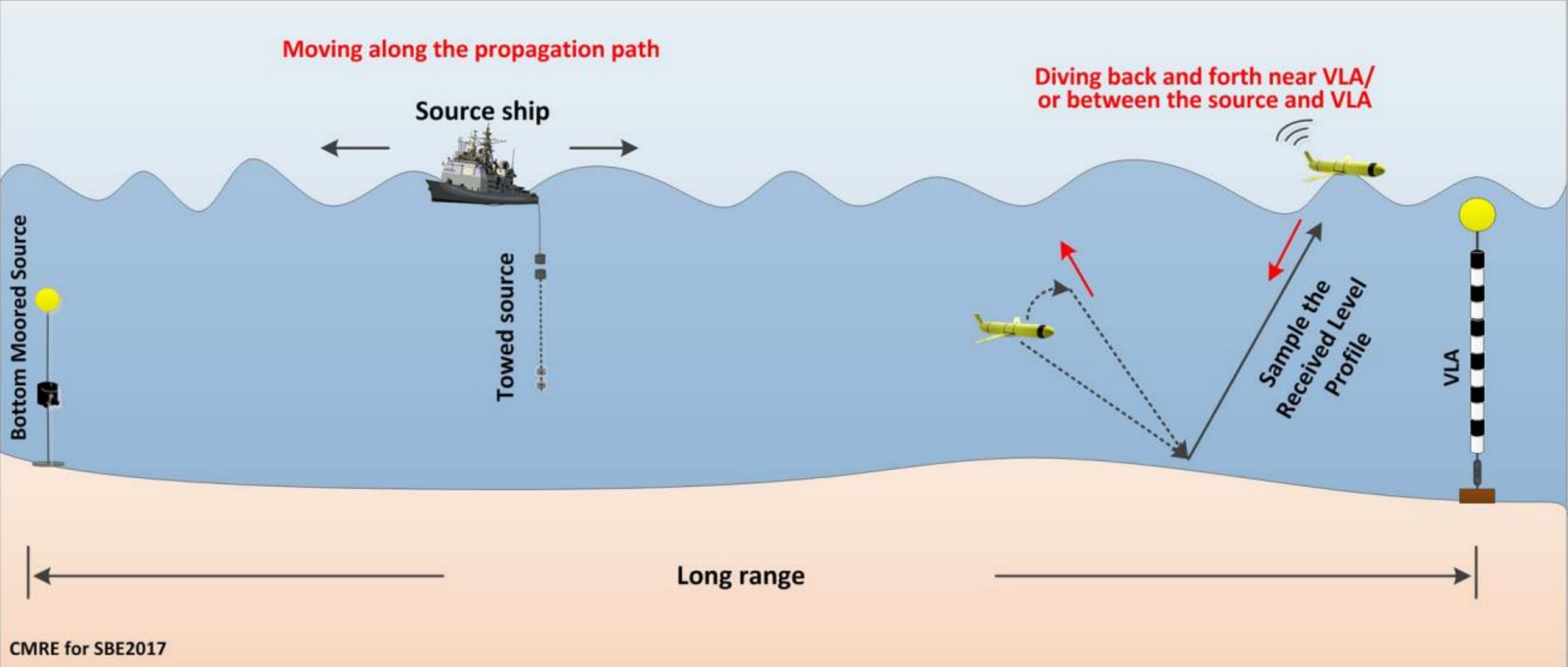
Seabed Type and Source Parameters Predictions Using Ship Spectrograms in Convolutional Neural Networks

Nazish Naeem

Ships of Opportunity (SOO)

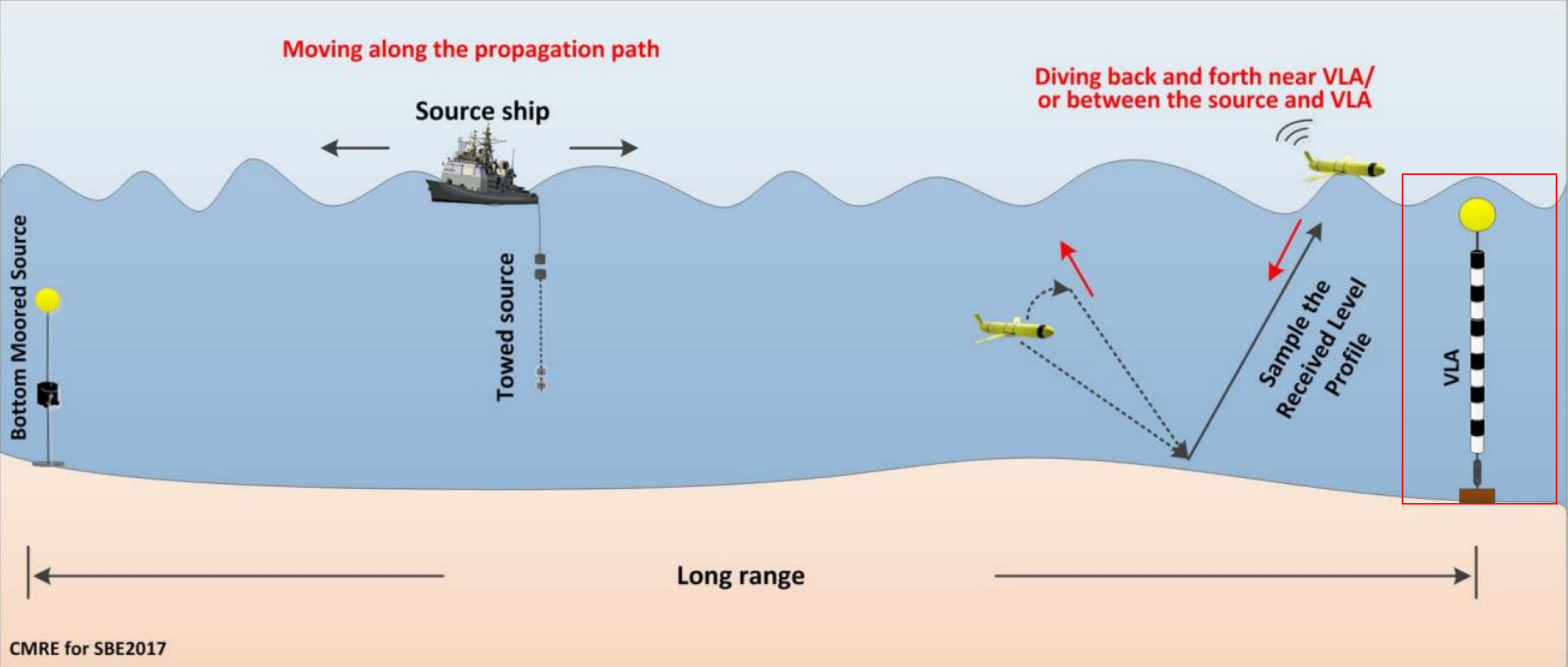
- Large container and oil tanker merchant ships produce **broadband noise**
- The noise is due to the highly **nonlinear** interaction between turbulence from the **ship hull** and **propeller**
- This noise propagates the **ocean waveguides** and thus have information about the seabed
- The received SOO noise can be used to infer the **seabed properties, closest point of approach (CPA) range and the ship speed**





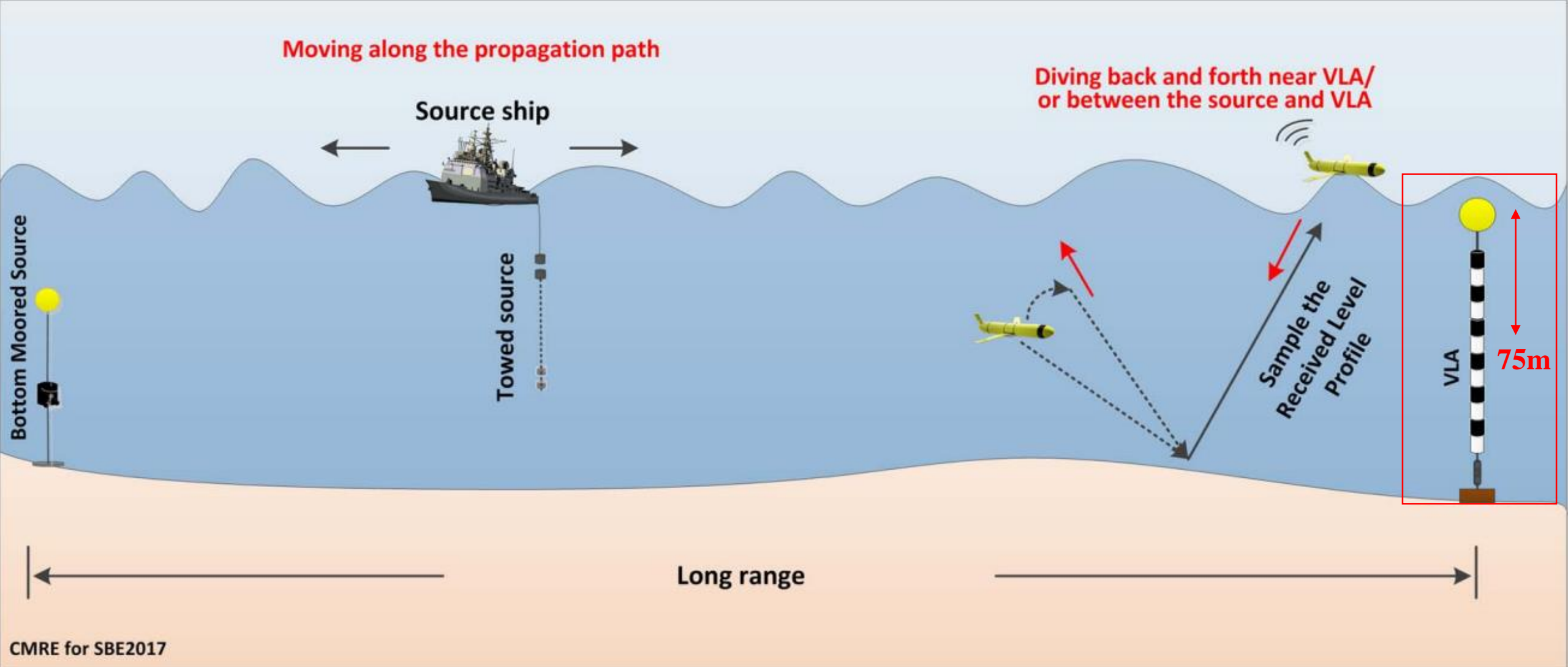
Available Dataset

- The data was recorded during SBCEX (SeaBed Characterization EXperiment) 2017 in the New England Mud-Patch
- The Kalamata container ship had a CPA to the VLA of 3.29km and was travelling at 19.9kn



Available Dataset

- The data was recorded during SBCEX (SeaBed Characterization EXperiment) 2017 in the New England Mud-Patch
- The Kalamata container ship had a CPA to the VLA of 3.29km and was travelling at 19.9kn



Available Dataset

- The data was recorded during SBCEX (SeaBed Characterization EXperiment) 2017 in the New England Mud-Patch
- The Kalamata container ship had a CPA to the VLA of 3.29km and was travelling at 19.9kn

Synthetic Data

Synthetic Data

$$S(f) = S_o - 10 \log(f^{3.594}) + 10 \log \left(\left(1 + \left(\frac{f}{340} \right)^2 \right)^{0.917} \right)$$

Synthetic Data

$$S(f) = S_o - 10 \log(f^{3.594}) + 10 \log \left(\left(1 + \left(\frac{f}{340} \right)^2 \right)^{0.917} \right)$$



Green's Function
(A range independent, normal mode
model for acousto-elastic ocean
environment)

Synthetic Data

$$S(f) = S_o - 10 \log(f^{3.594}) + 10 \log \left(\left(1 + \left(\frac{f}{340} \right)^2 \right)^{0.917} \right)$$



- Seabed type
- Ship Speed
- CPA
- Effective ship source depth and Sound Speed Profile (SSP)



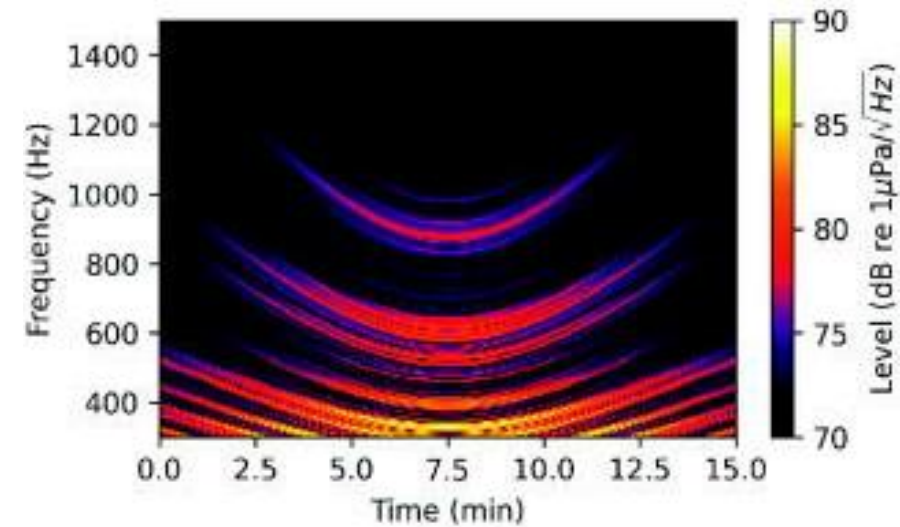
Green's Function
(A range independent, normal mode model for acousto-elastic ocean environment)

Synthetic Data

$$S(f) = S_o - 10 \log(f^{3.594}) + 10 \log \left(\left(1 + \left(\frac{f}{340} \right)^2 \right)^{0.917} \right)$$

- Seabed type
- Ship Speed
- CPA
- Effective ship source depth and Sound Speed Profile (SSP)

Green's Function
(A range independent, normal mode model for acousto-elastic ocean environment)



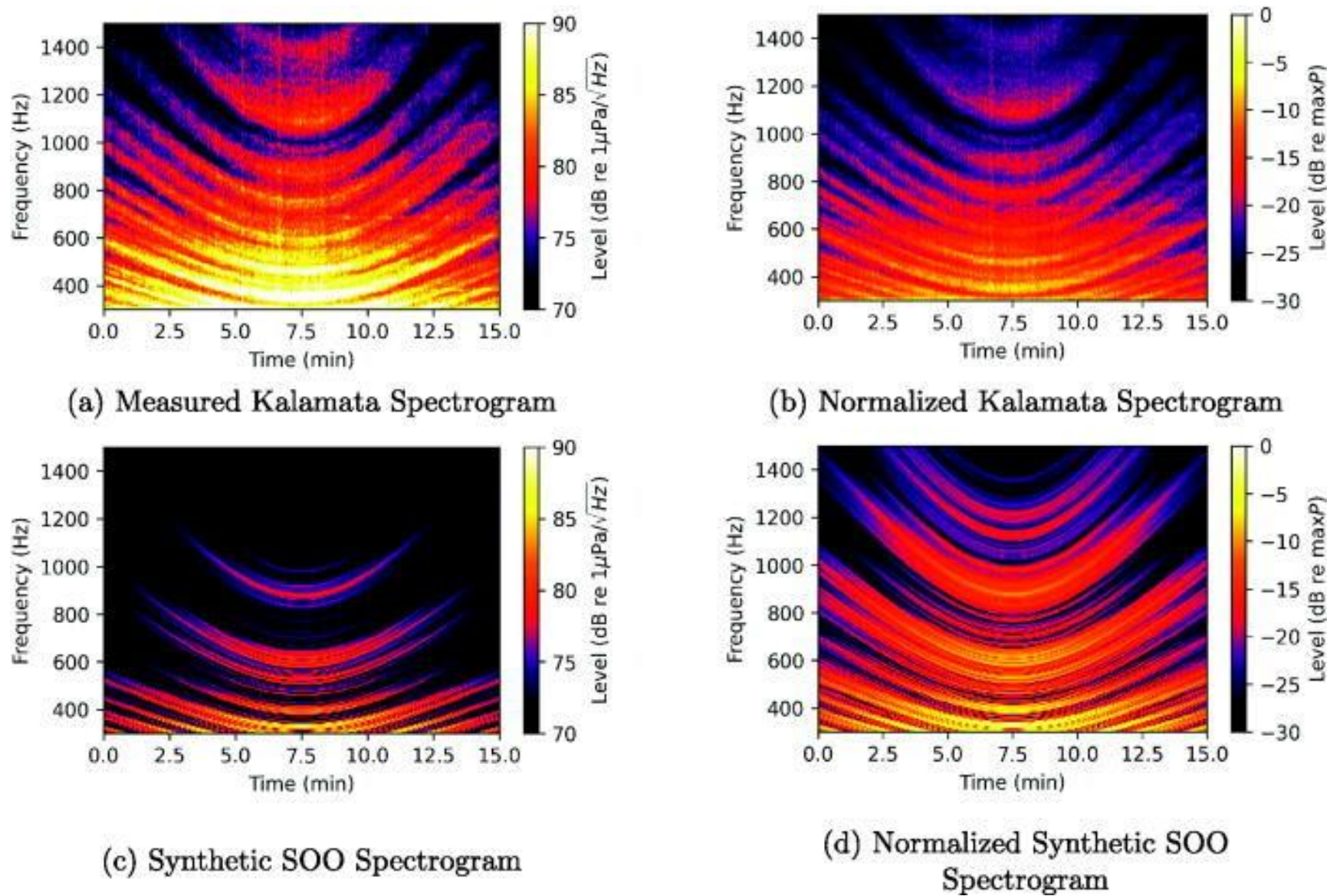


FIG. 1. (Color online) Example SOO spectrograms. (a) Absolute and (b) normalized spectrograms of the Kalamata measured on channel 8 of the Marine Physical Laboratory of the Scripps Institution of Oceanography (MPL) VLA 2 during SBCEX 2017. (c) Absolute and (d) normalized synthetic spectrograms for a ship traveling 20.0 kn with a CPA of 3.3 km—similar to the Kalamata—using the mud-over-sand seabed type. The “normalized” spectrograms use the maximum pressure of the spectrogram as the reference instead of $1 \mu\text{Pa}$.

Training Dataset

- 4 Seabed types (deep mud, mud-over-sand, sandy-silt and sand) were used
- 50 different sound speeds were used in combination with all seabed types making 200 ocean environments
- 9 ship speeds, 9 CPA ranges and two source depths were selected for each 200 environments.
- 32400 samples for training

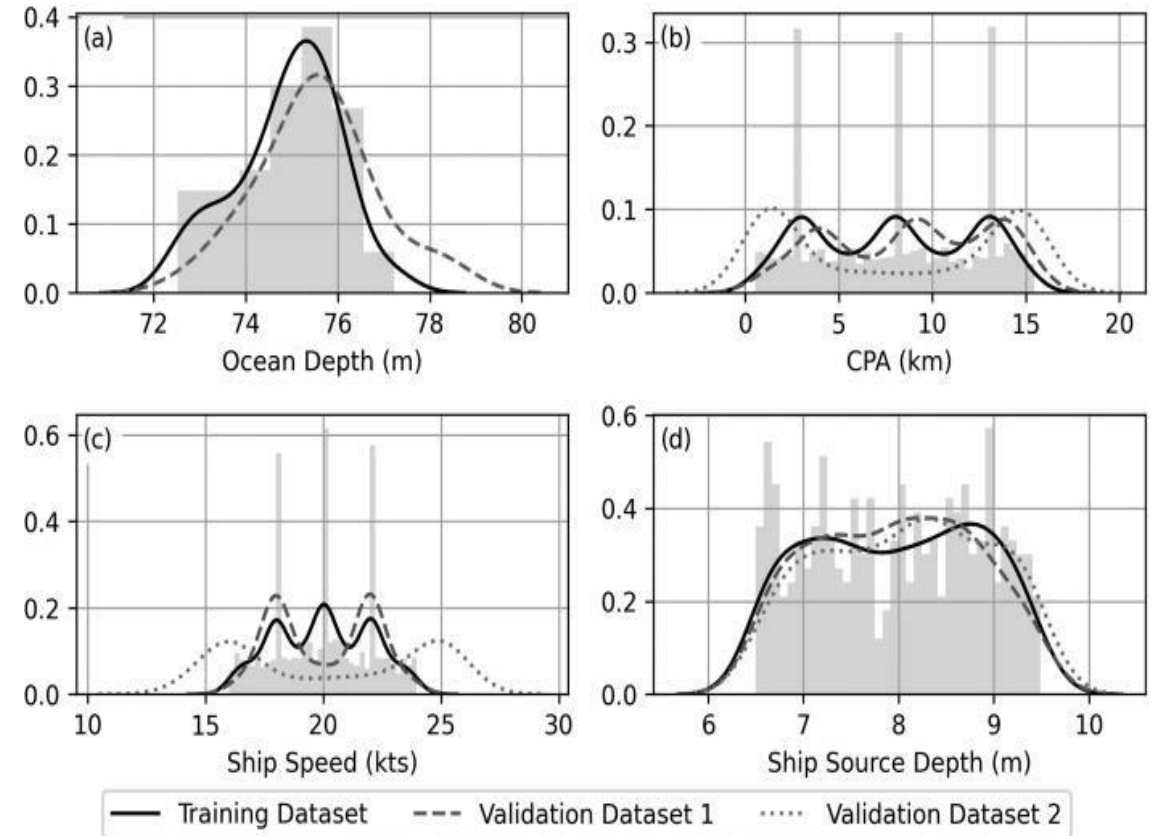
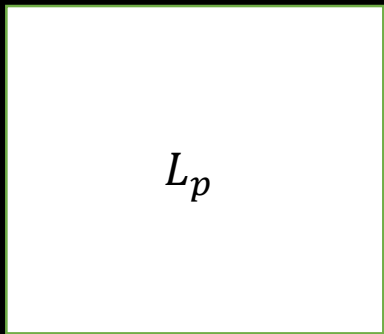
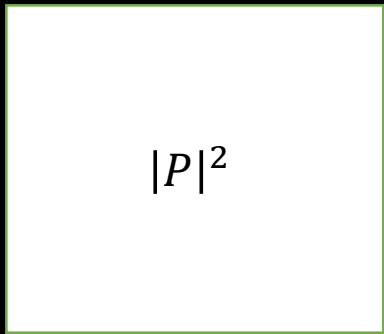
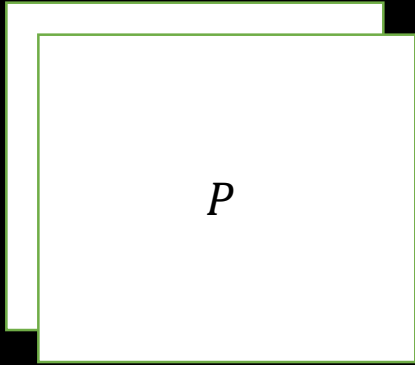
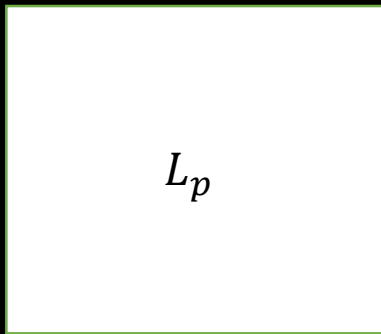
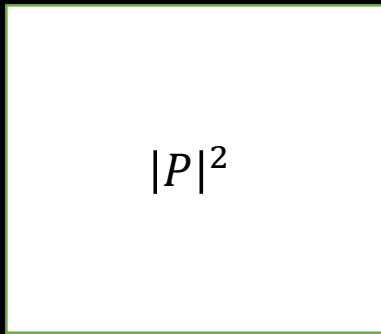
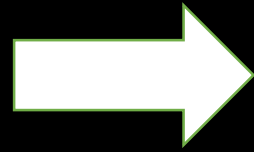
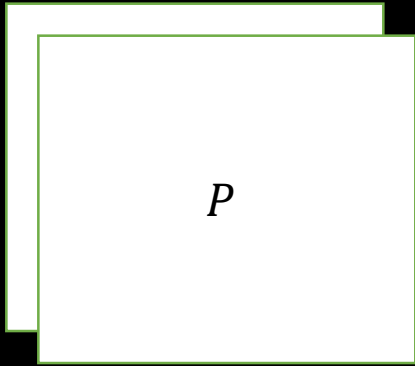
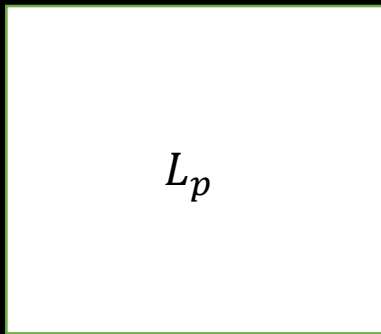
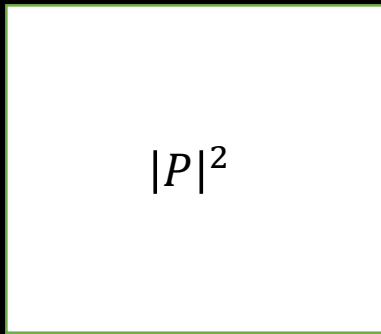
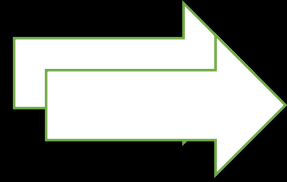
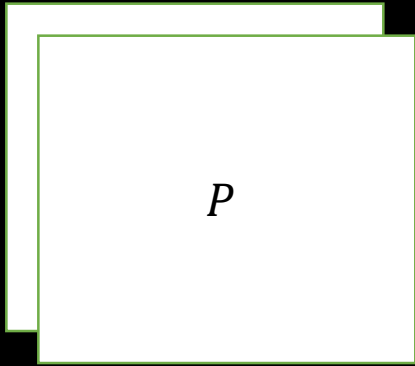
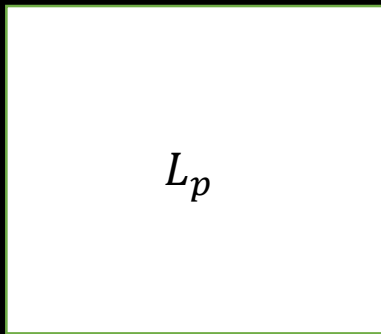
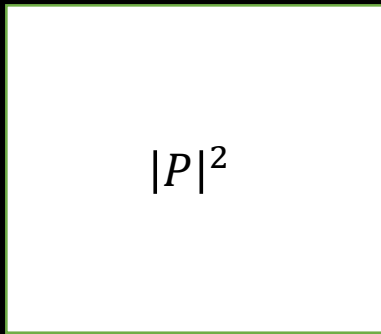
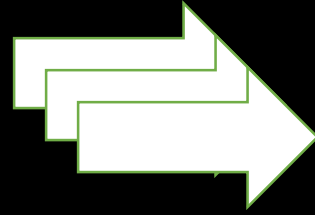
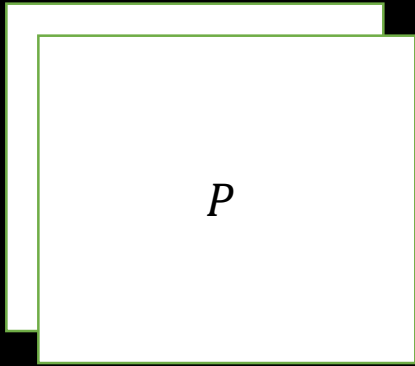


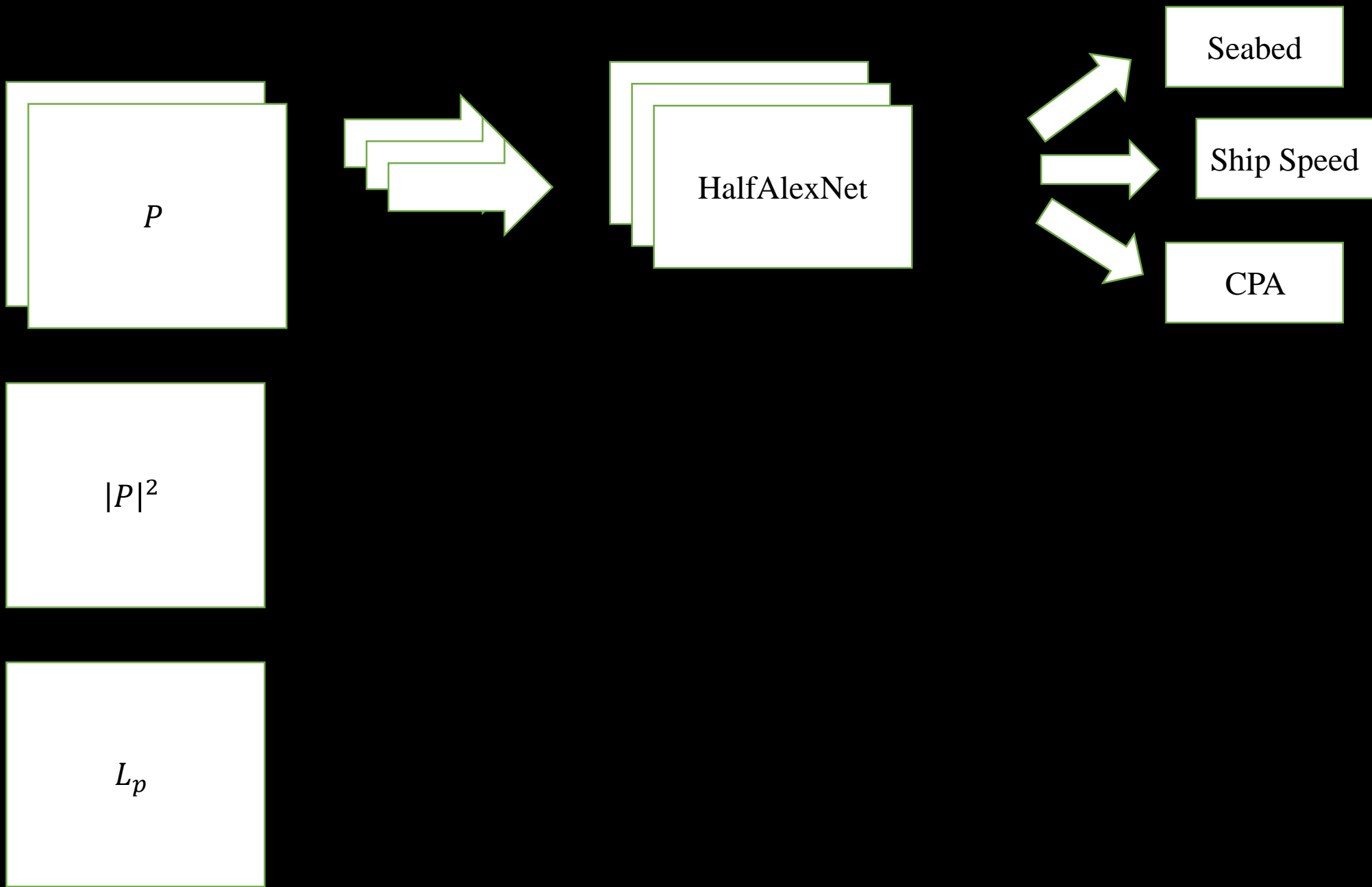
FIG. 2. Normalized histograms (shaded gray areas) and kernel density estimates (solid lines) of the random parameters selected for the training dataset. (a) Ocean depths over the 50 SSPs, (b) CPA ranges, (c) ship speeds, and (d) source depths over the 200 environments. The large peaks correspond to values that were selected for each environment. The dashed and dotted lines represent the kernel density estimates of the various parameters for the two validation sets.

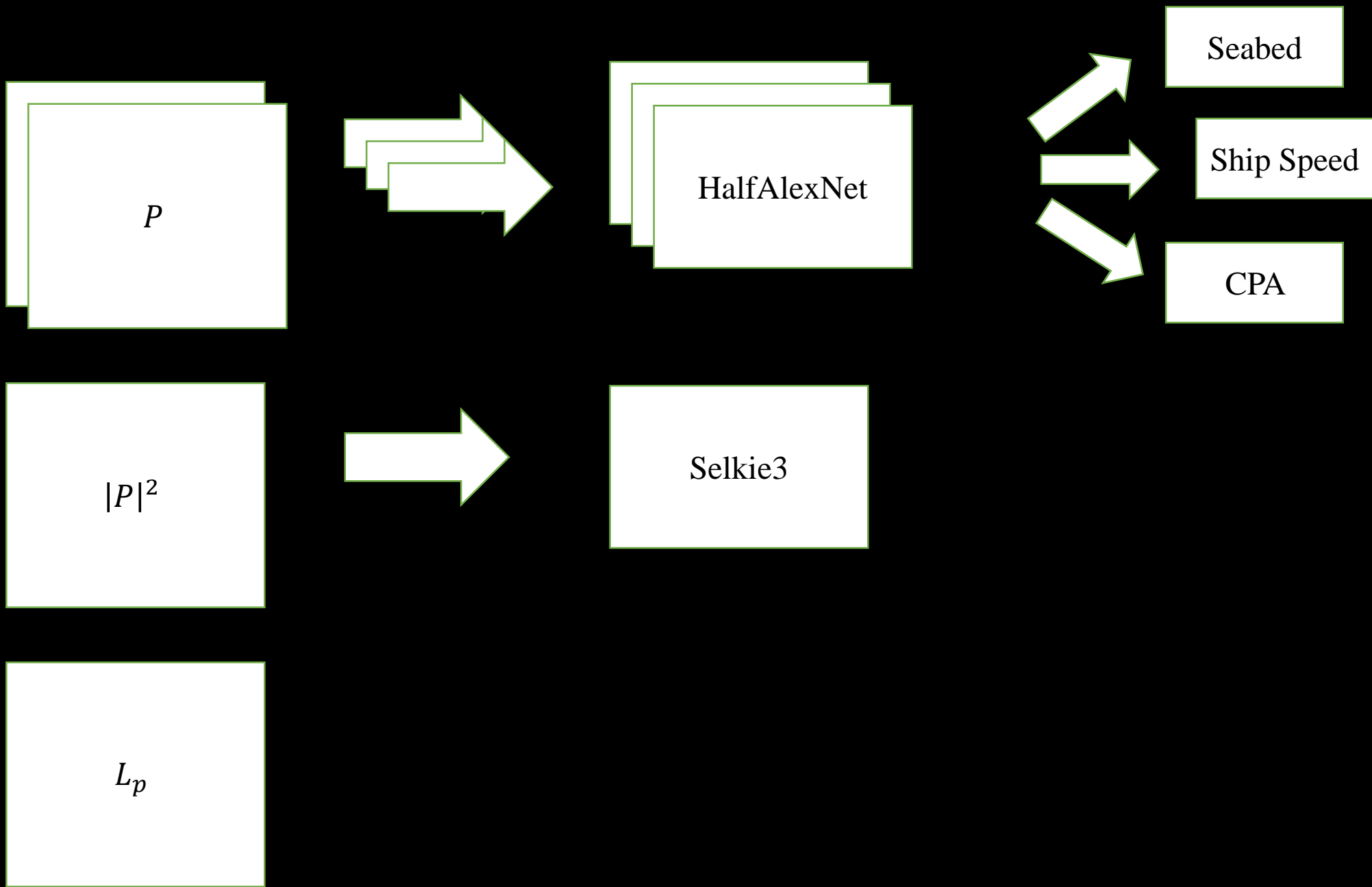


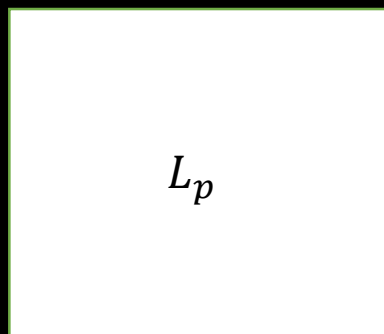
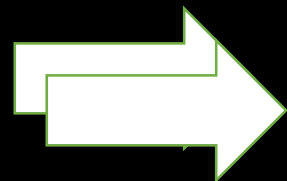
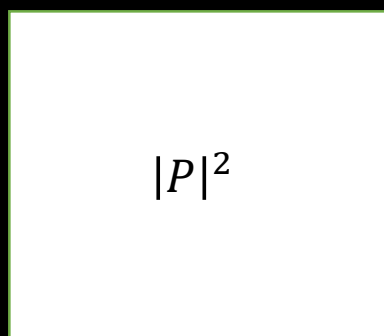
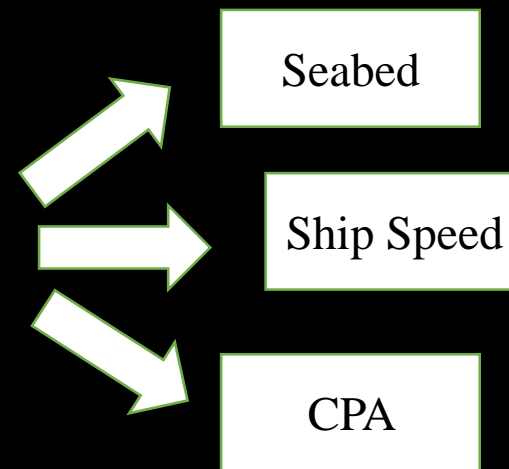
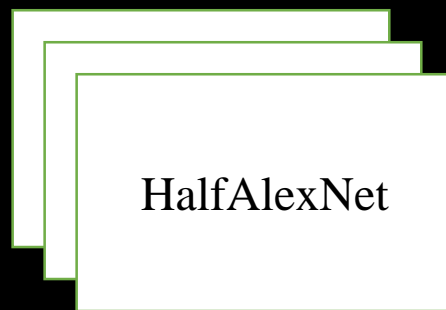
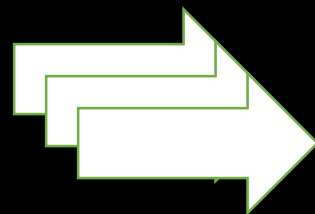
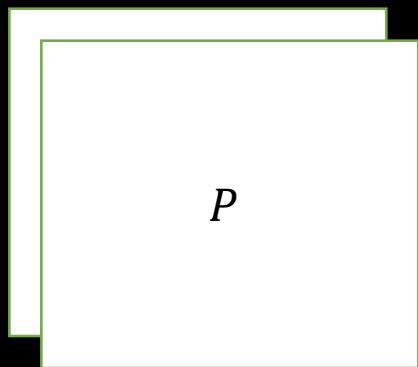


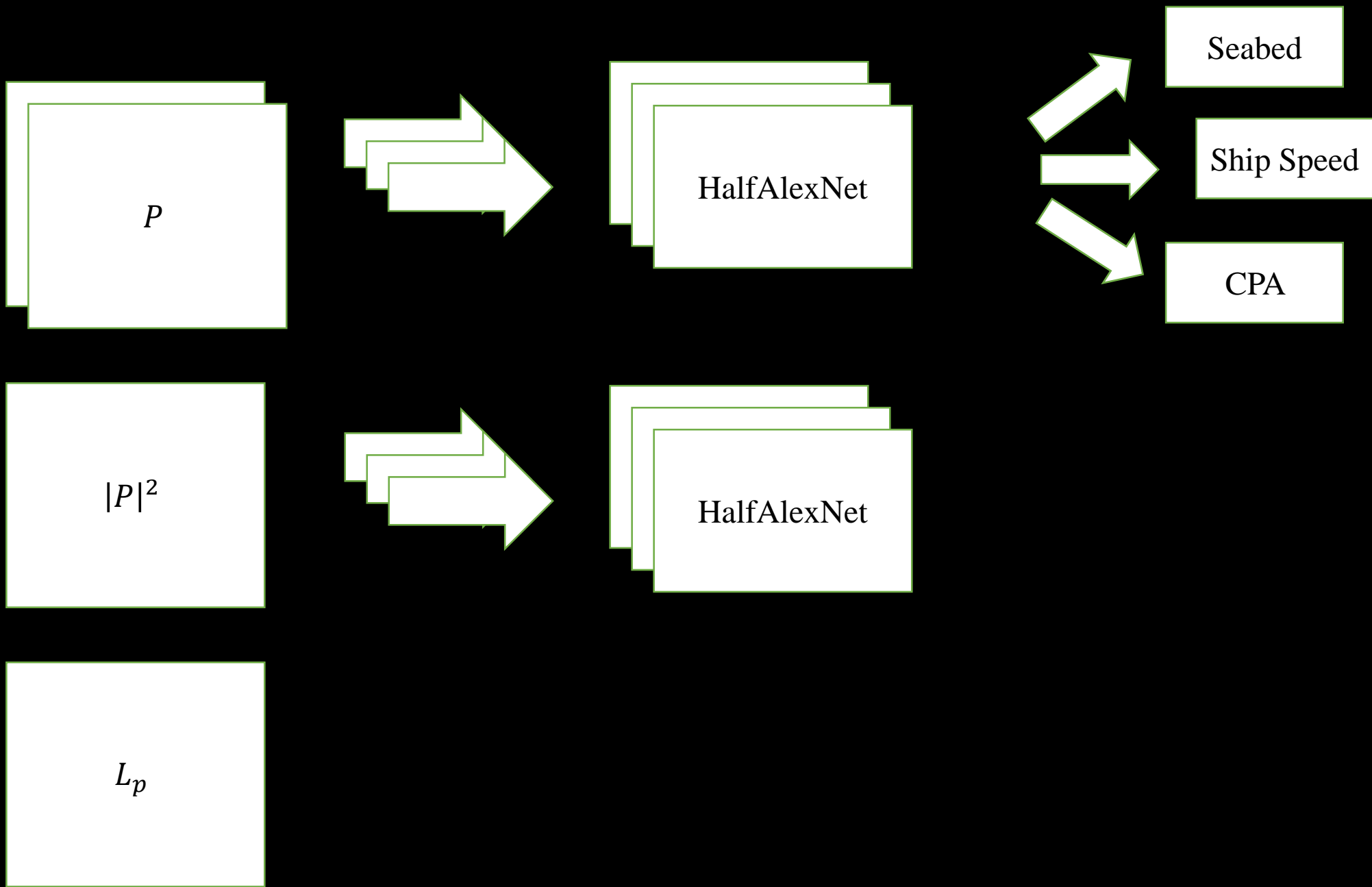


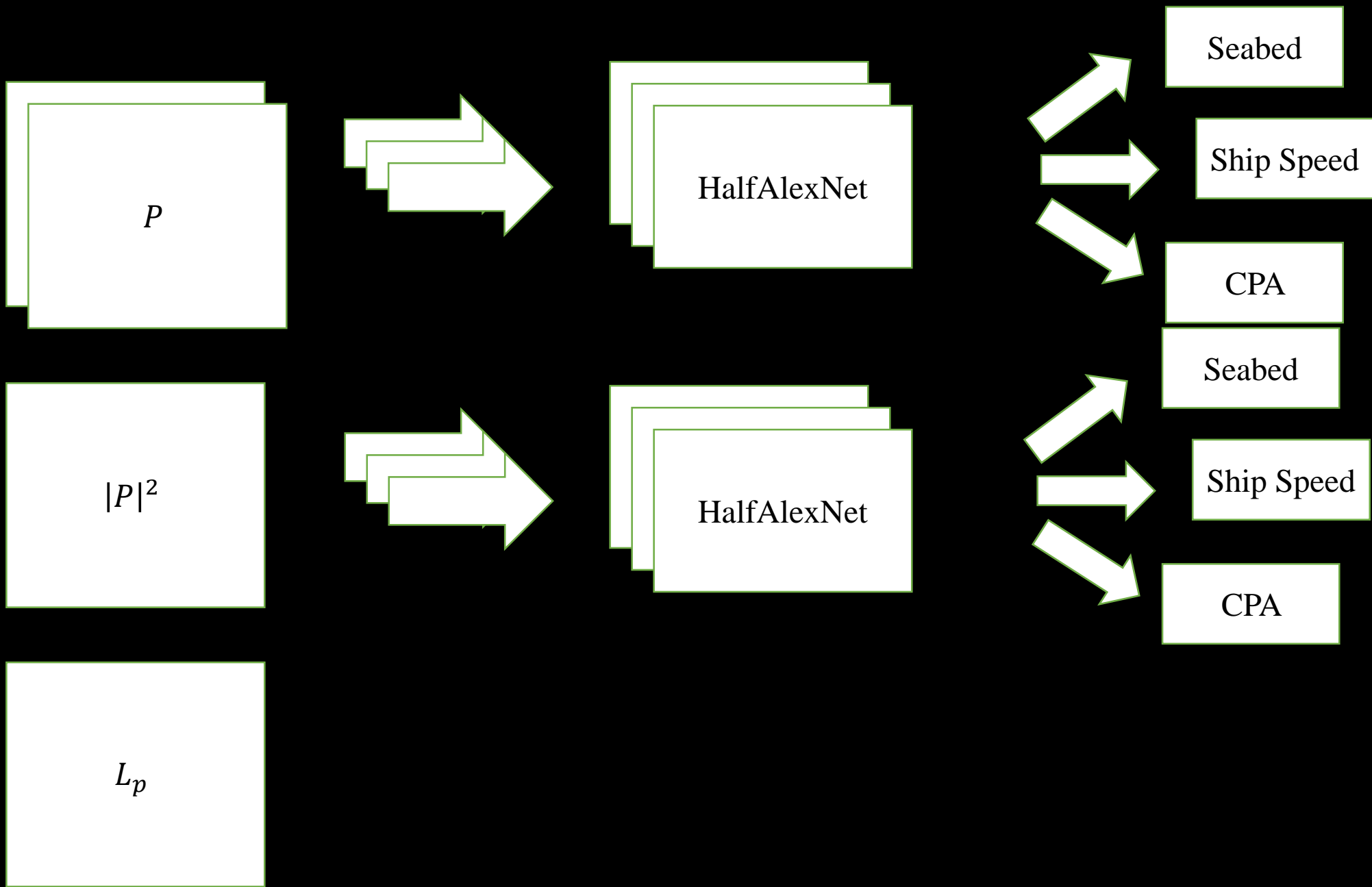


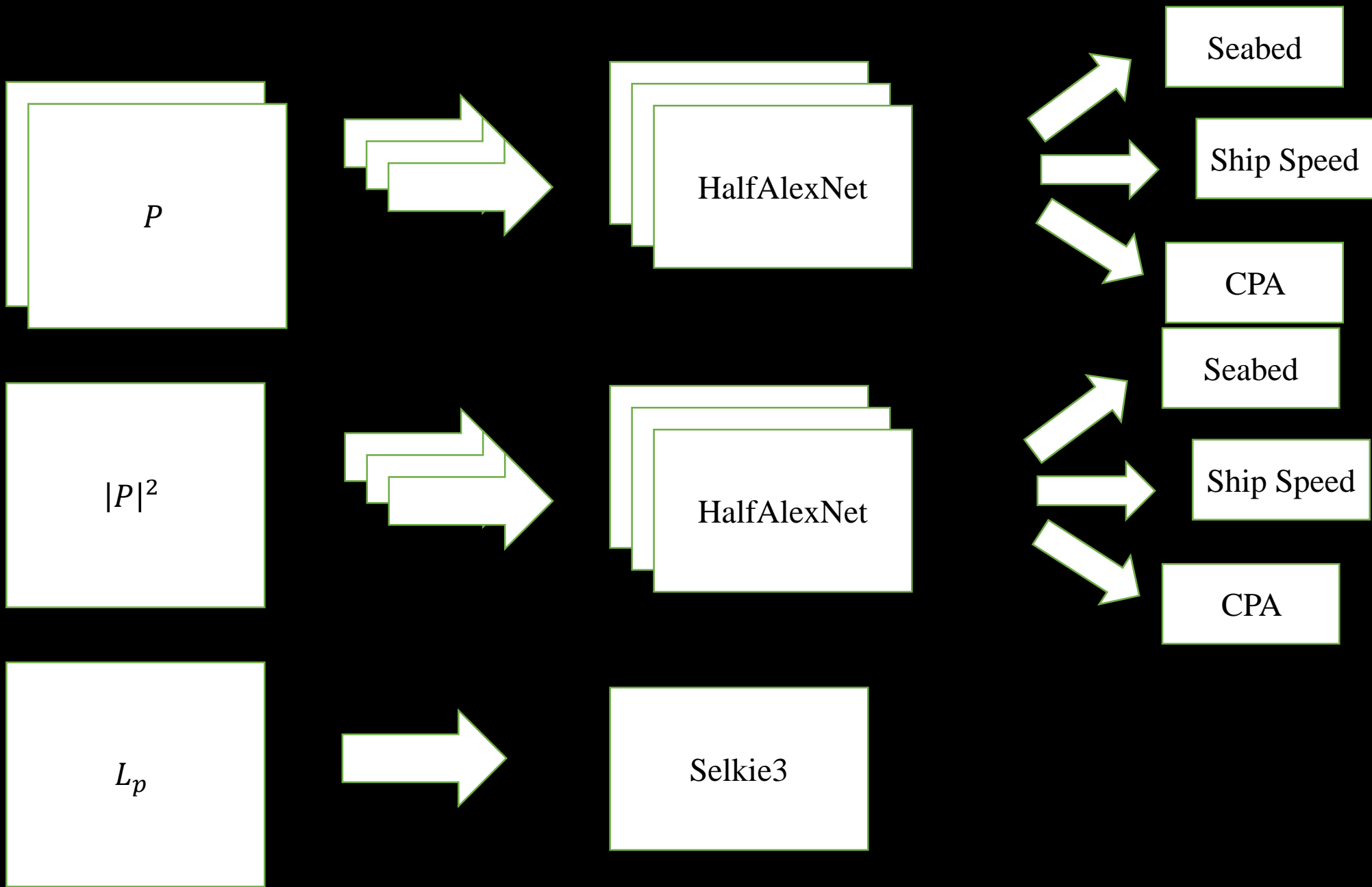


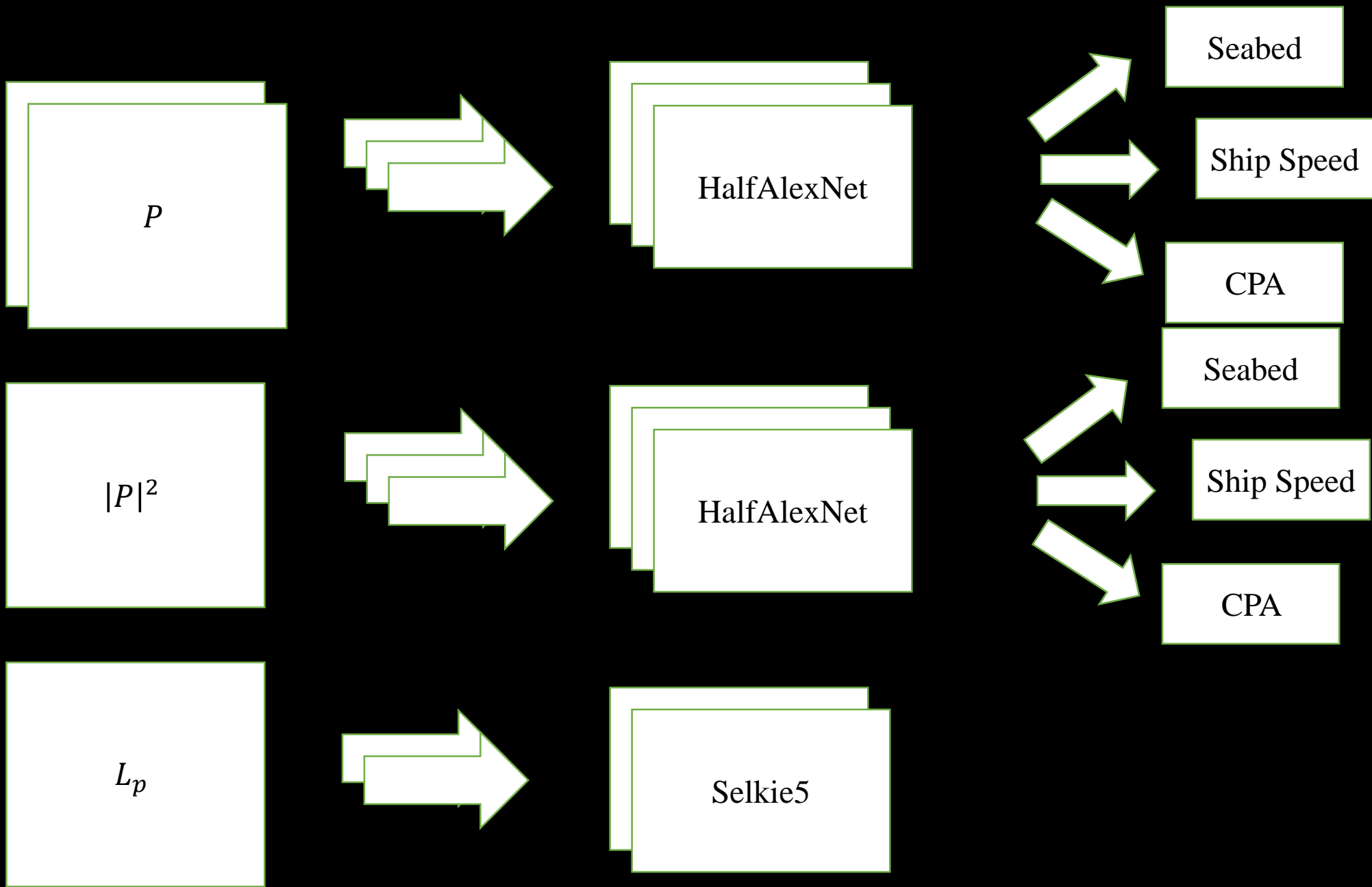


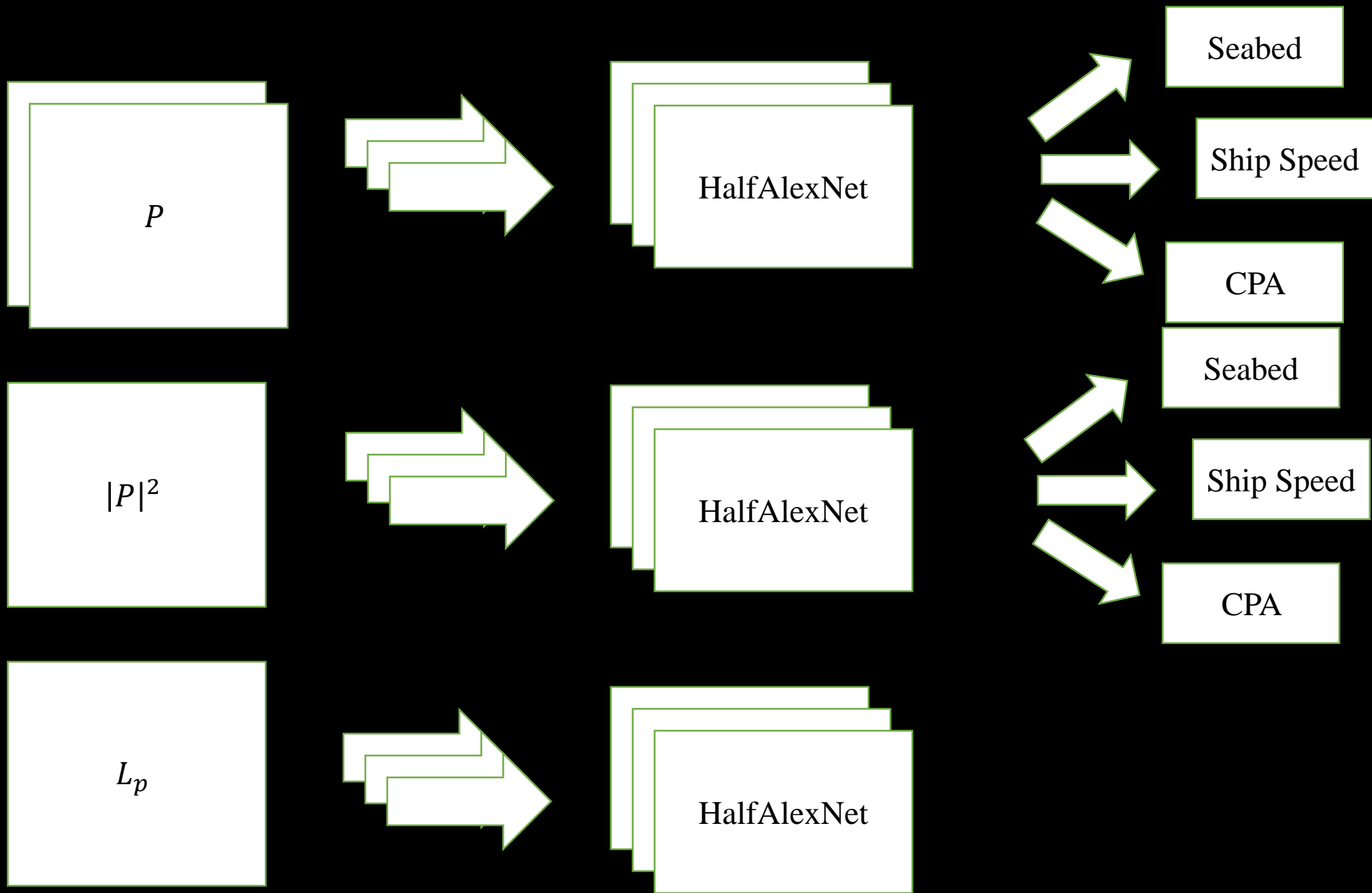


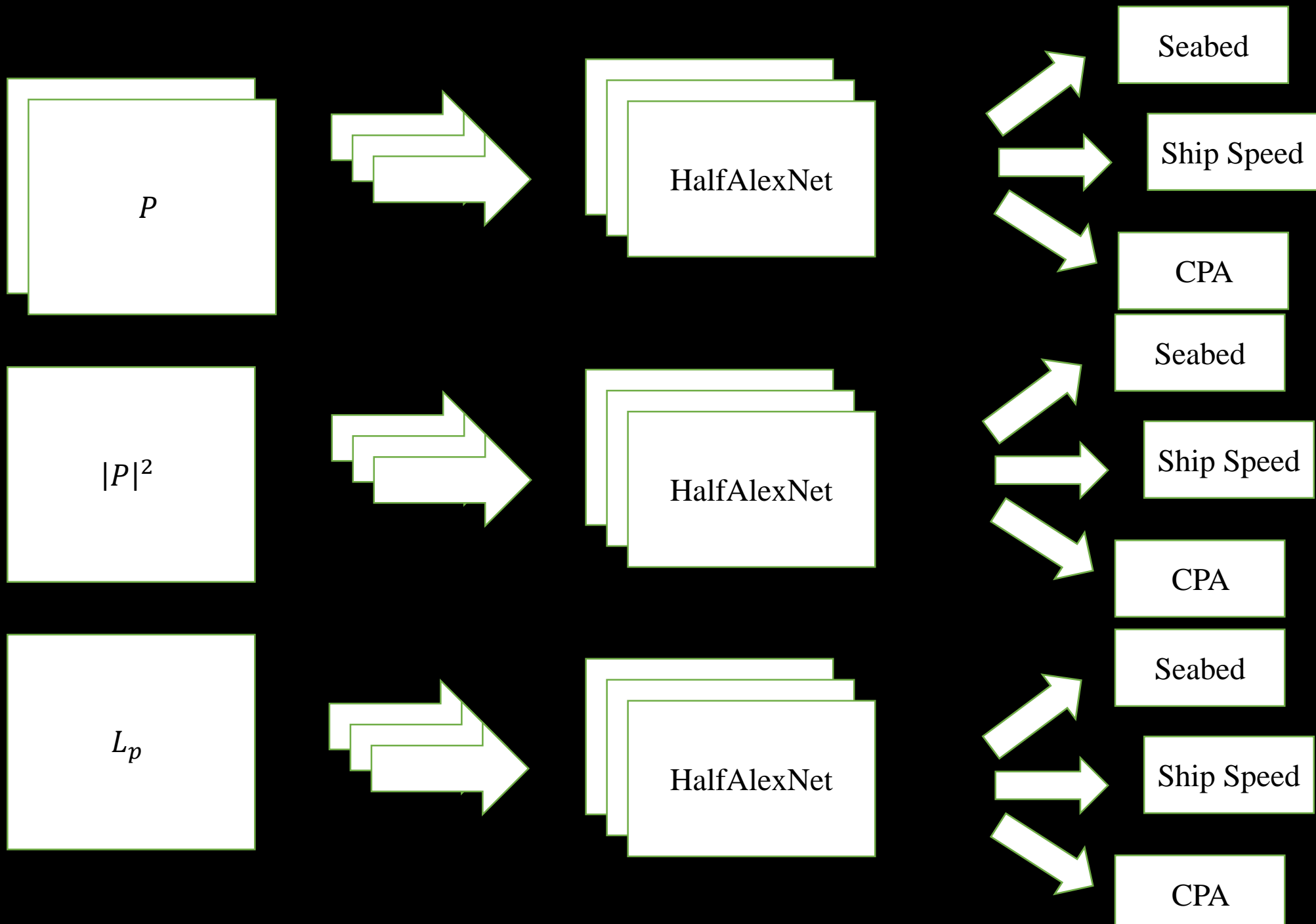




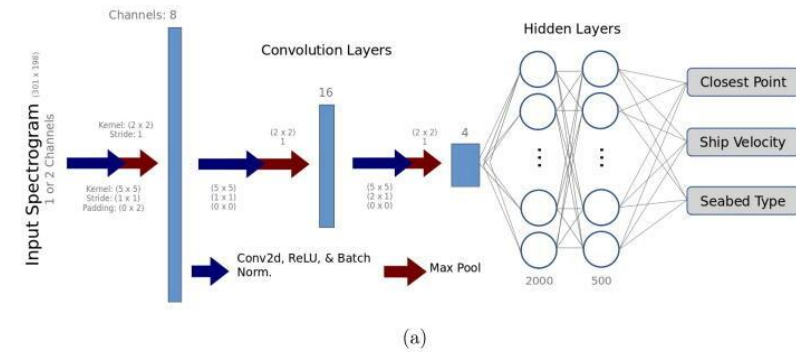






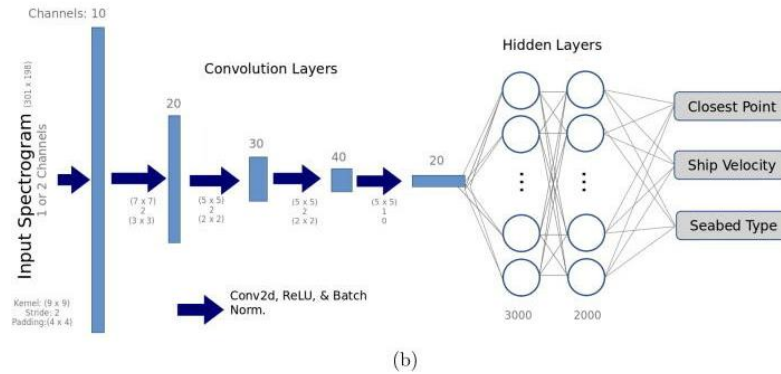


Selkie 3



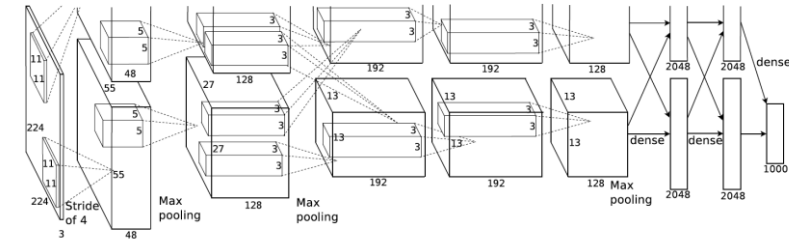
4.3M learnable parameters

Selkie 5



14.2M learnable parameters

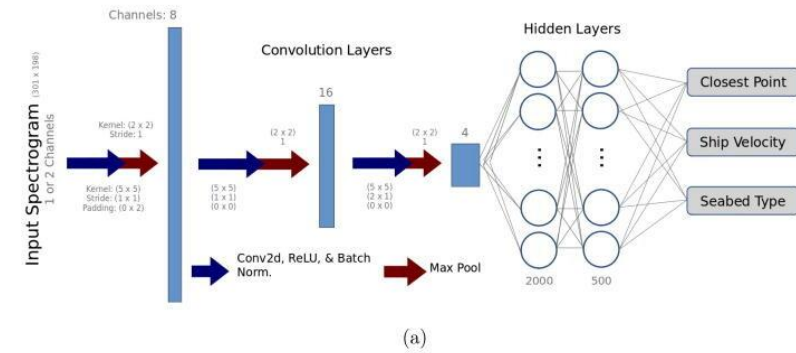
HalfAlexNet



15.6M learnable parameters

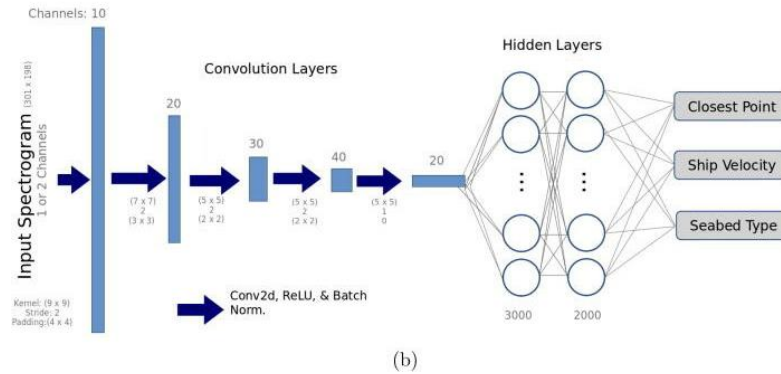
CNN Topology

Selkie 3



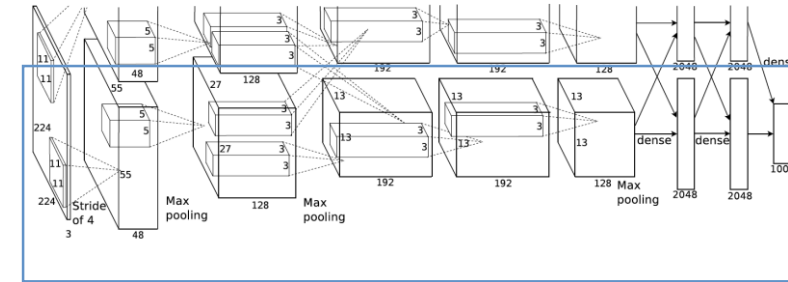
4.3M learnable parameters

Selkie 5



14.2M learnable parameters

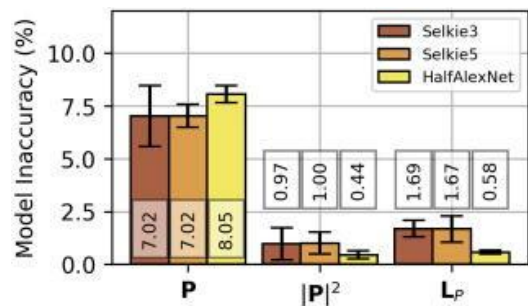
HalfAlexNet



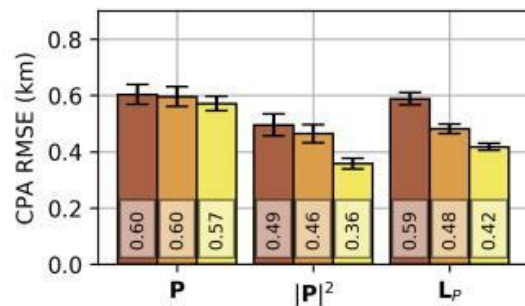
15.6M learnable parameters

CNN Topology

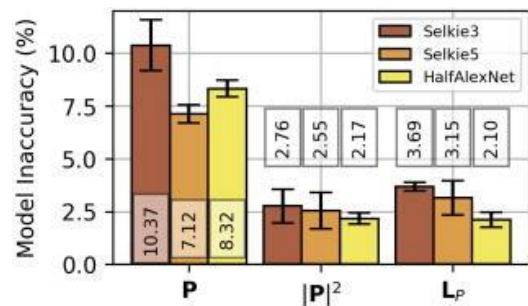
Results



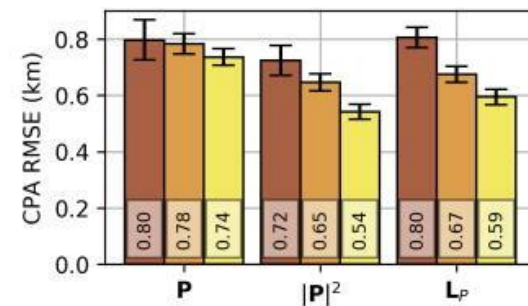
(a) Seabed Errors



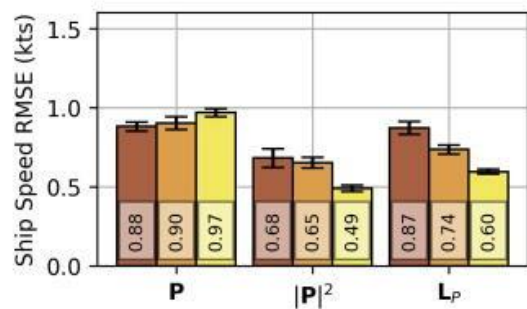
(b) CPA Errors



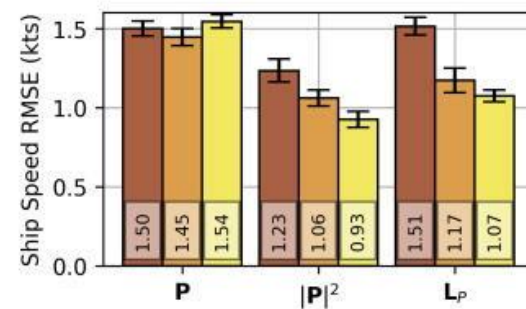
(a) Seabed Errors



(b) CPA Errors



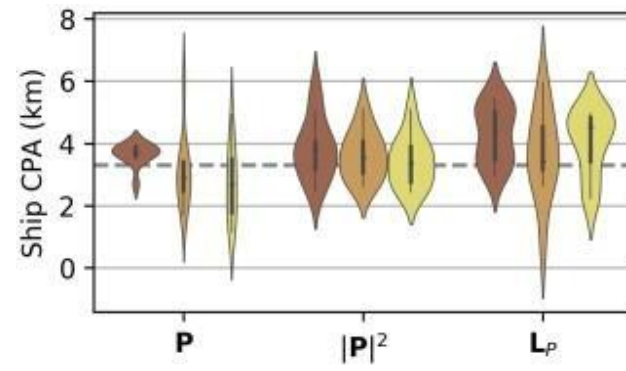
(c) Speed Errors



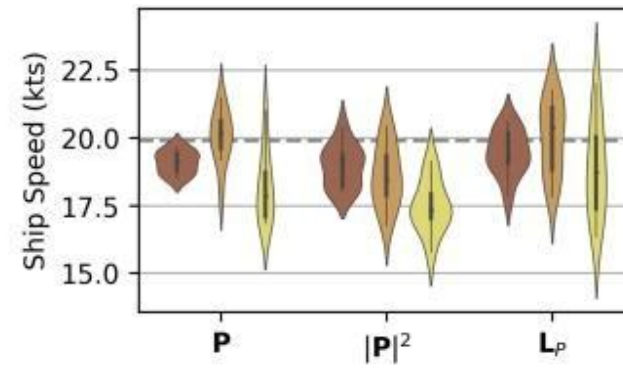
(c) Speed Errors

FIG. 5. (Color online) Results from ten training instances of each network on validation dataset 1 containing 5400 samples and designed to test the ability of the networks to interpolate

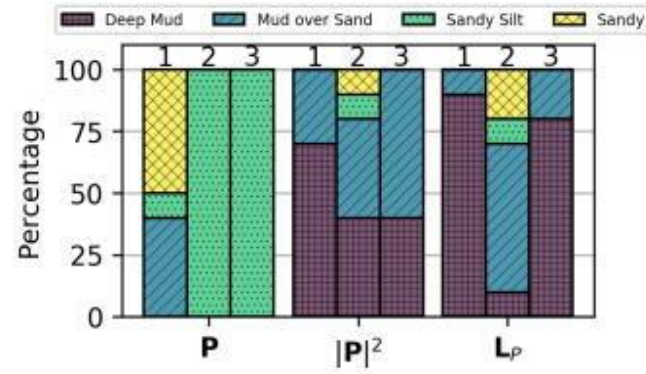
FIG. 6. (Color online) Results from ten training instances of each network on validation dataset 2 containing 8640 samples and designed to test the ability of the networks to extrapolate



(a) CPA Predictions



(b) Speed Predictions



(c) Seabed Predictions

FIG. 7. (Color online) Results from ten instances of each network on the measured Kalamata spectrogram. Violin plots (a normalized probability distribution kernel with the median and quartile ranges over the ten training instances) of (a) the CPA range and (b) the speed predictions. (c) Stacked barchart showing the percentage of predictions for each seabed type. The input data type is listed on the horizontal axis. The three networks are distinguished by color in (a) and (b), similar to Figs. 5 and 6, and by numbers on top of the bars in (c) with 1 = Selkie3, 2 = Selkie5, and 3 = HalfAlexNet.

Observations:

Observations:

- The differences in the results based on input type is larger than differences due to the network type

Observations:

- The differences in the results based on input type is larger than differences due to the network type
- Larger networks perform better on validation dataset while the smaller network performs better on the test data

Observations:

- The differences in the results based on input type is larger than differences due to the network type
- Larger networks perform better on validation dataset while the smaller network performs better on the test data
- The learned weights of the linear layers of the network as the number of neurons increase, become smaller and overfit on the training dataset distribution

Observations:

- The differences in the results based on input type is larger than differences due to the network type
- Larger networks perform better on validation dataset while the smaller network performs better on the test data.
- The learned weights of the linear layers of the network as the number of neurons increase, become smaller and overfit on the training dataset distribution
- The use of ship spectrogram in neural networks is a promising tool for ocean acoustics

Observations:

- The differences in the results based on input type is larger than differences due to the network type
- Larger networks perform better on validation dataset while the smaller network performs better on the test data
- The learned weights of the linear layers of the network as the number of neurons increase, become smaller and overfit on the training dataset distribution
- The use of ship spectrogram in neural networks is a promising tool for ocean acoustics
- This preliminary study can be expanded by introducing more variables and random noise representative of the ambient or wind noise in the synthetic data